and $SiCl_3$-like species (*11*). This enhanced splitting is consistent with the greater orbital overlap and bond strength of Si–Cl bonds compared to Si–Si bonds. A similar trend has been reported for the analogous hydride species present on both the hydrogenated Si(111)-(7×7) and amorphous Si surfaces (*12, 13*). Based on these results we suggest that the intensity of both the backbond state and the tail of the σ^* state that extends into the tunneling energy window depends on the adatom species from which they are derived, both being more pronounced for those that contain fewer Cl atoms. This behavior is directly reflected in the topographs of Fig. 2, where in order to maintain the required stabilization current the tip-to-surface distance must decrease as the number of Cl atoms bonded to the adatom increases.

Although reacted and unreacted db sites can be readily distinguished with the use of *I-V* curves (*6, 9*), we were unable to distinguish between the different chlorinated adatoms with this method. The differences in the latter case are subtle and involve changes in the shape of the background. The problem arises from the presence of bulk states that dominate the *I-V* curves and mix with and broaden the states of interest. Furthermore, *I-V* curves recorded at a given site on the surface are normalized to the current at that site (*1*), making it difficult to compare the shape and size of the backgrounds at different surface sites. Despite this, the different products known to exist on this surface can be distinguished on the basis of their registry and appear as adatoms of different sizes consistent with the number of Si–Si and Si–Cl bonds they contain.

REFERENCES AND NOTES

1. R. M. Feenstra, J. A. Stroscio, A. P. Fein, *Surf. Sci.* **181**, 295 (1986).
2. See, for example, H. Ohani, R. J. Wilson, S. Chang, C. M. Mate, *Phys. Rev. Lett.* **60**, 2398 (1988).
3. J. E. Demuth, R. J. Hamers, R. M. Tromp, M. E. Welland, *J. Vac. Sci. Technol. A* **4**, 1320 (1986).
4. R. D. Schnell, D. Rieger, A. Bogen, K. Wandelt, W. Steinmann, *Solid State Commun.* **53**, 205 (1985).
5. K. Takayanagi, Y. Tanishiro, S. Takahashi, M. Takahashi, *Surf. Sci.* **164**, 367 (1985).
6. J. J. Boland and J. S. Villarrubia, *Phys. Rev. B*, in press.
7. R. D. Schnell *et al.*, *ibid.* **32**, 8057 (1985).
8. J. S. Villarrubia and J. J. Boland, *Phys. Rev. Lett.* **63**, 306 (1989).
9. R. Wolkow and Ph. Avouris, *ibid.* **60**, 1049 (1988).
10. M. Schlüter and M. L. Cohen, *Phys. Rev. B* **17**, 716 (1978).
11. J. J. Boland and A. Rossi, unpublished results.
12. K. M. Ho, M. L. Cohen, M. Schlüter, *Phys. Rev. B* **15**, 3888 (1977).
13. B. von Roedern, L. Ley, M. Cardona, F. W. Smith, *Philos. Mag. B* **40**, 433 (1979).
14. We thank A Rossi for assistance with the calculations and J. Baker for use of his curve-fitting software.

24 January 1990; accepted 4 April 1990

Electro-Optical Evidence for the Chelate Effect at Semiconductor Surfaces

GEORGE C. LISENSKY,* RONA L. PENN, CATHERINE J. MURPHY, ARTHUR B. ELLIS*

Monoamines and diamines dissolved in cyclohexane solution reversibly enhance the band-edge photoluminescence (PL) intensity of immersed n-type cadmium sulfide (n-CdS) and n-type cadmium selenide (n-CdSe) substrates through adsorption. The magnitude of the PL increase is used to estimate amine-induced contractions in the semiconductor's depletion width, and the dependence of the PL intensity on amine concentration provides an estimate of the adduct formation constant. Two diamines, ethylenediamine and *o*-phenylenediamine, exhibit unusually low reductions in depletion width and substantially larger adduct equilibrium constants relative to the other amines studied, consistent with chelation to surface Cd^{2+} ions. These studies demonstrate that PL can be used as a contactless, in situ technique for characterizing the steric and electronic landscape of semiconductor surfaces and for correlating molecular and surface chemistry.

DESPITE THE IMPORTANCE OF SURFACE chemistry in semiconductor technology, its role in determining the electro-optical characteristics of semiconductor materials is not well understood (*1*). We have embarked on a program to characterize the surface chemistry of the II-VI semiconductors n-CdS and n-CdSe. Using the bandgap PL of the solid as a probe, we have characterized surface adduct formation with amines and butenes in the gas phase and with phosphines and lanthanide β-diketonate complexes in hydrocarbon solution (*2–5*).

In this report, we establish a link between classical coordination chemistry and surface chemistry by demonstrating chelation at the semiconductor-solution interface. The "chelate effect" refers to the enhanced stability of a coordination compound containing polydentate ligands relative to one with analogous monodentate ligands (*6*). An example of this effect is provided by the following comparison of displacement reactions in aqueous solution, where β_n is the overall formation constant for *n* ligands coordinated to the metal center, for which the bidentate amine has the larger formation constant (*7*):

$$Cd^{2+}(aq) + 4CH_3NH_2 \rightarrow Cd(CH_3NH_2)_4{}^{2+}, \log \beta_4 = 6.52 \quad (1)$$

$$Cd^{2+}(aq) + 2H_2NCH_2CH_2NH_2 \rightarrow Cd(H_2NCH_2CH_2NH_2)_2{}^{2+}, \log \beta_2 = 10.6 \quad (2)$$

That surface atoms could form part of a chelate ring with solution species has been hypothesized in several studies (*8*), including ones involving adsorption of dithiocarbamates from CH_3CN solution and of EDTA from aqueous solution onto CdS or CdSe (*9*). We provide evidence here from PL data that diamines can chelate to surface-lattice Cd^{2+} ions by adsorption from cyclohexane solution. Signatures of chelation are a smaller perturbation of the semiconductor's depletion [because of the low density of charge carriers in a semiconductor, the electric field, which results from charge trapped at the solid's surface, extends for some distance, known as the depletion width, into the solid (*10*)] and far larger adduct formation constants than are found for monoamines of comparable size. Our data also highlight the general use of PL as a contactless, in situ technique for characterizing semiconductor-derived interfaces.

We have focused on amines in this study because they form stable Cd^{2+} complexes (Eqs. 1 and 2). The diamines selected for study include ethylenediamine (en), *o*-phenylenediamine (opda), and 1,3-propanediamine (tn), which are almost always found

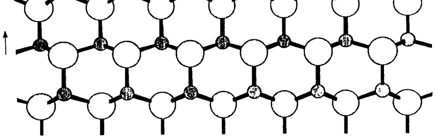

Fig. 1. Possible modes of en bonding are shown: from left to right, chelating, bridging, and monodentate bonding. The smaller circles represent Cd^{2+} sites; the larger circles represent S^{2-} or Se^{2-} sites. The 0001 face of CdS (or CdSe) is perpendicular to the plane of the figure, and the crystallographic *c* axis is indicated.

G. C. Lisensky and R. L. Penn, Department of Chemistry, Beloit College, Beloit, WI 53511.
C. J. Murphy and A. B. Ellis, Department of Chemistry, University of Wisconsin–Madison, Madison, WI 53706.

*To whom correspondence should be addressed.

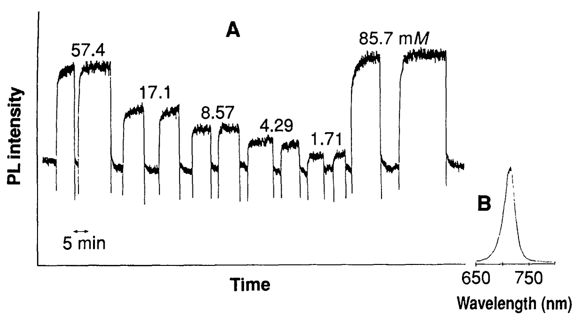

Fig. 2. (**A**) Changes in PL intensity at 720 nm resulting from alternating exposure of an etched n-CdSe sample to cyclohexane (initial and alternate responses) and to various concentrations of 1,6-hexanediamine in cyclohexane. Downward spikes are caused by the draining of the cell under N_2 when the solutions were changed. (**B**) The final PL spectrum, obtained in cyclohexane, shows the baseline. The sample was excited with 457.9-nm light in both cases.

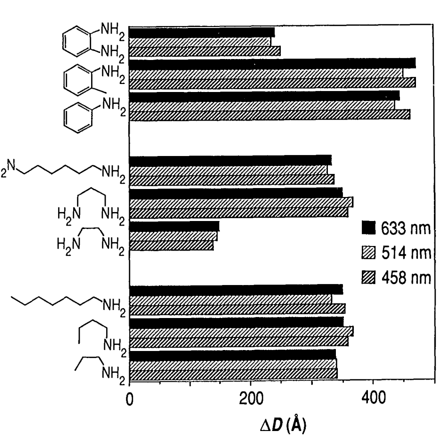

Fig. 3. Values of ΔD for a single CdSe sample with each of the amines examined, calculated with Eq. 3. A pooled estimate of the standard deviation in ΔD is 20 Å (15 df). Other appropriately etched samples give similar responses. Excitation wavelengths are shown in the legend. The dead-layer model predicts that ΔD will be independent of excitation wavelength for a given analyte. Penetration depths ($1/\alpha$ of 570, 740, and 1500 Å at 457.9, 514.5 and 632.8 nm, respectively) and the correction for self-absorption ($\beta = 1.2 \times 10^4$ cm^{-1}) were obtained from Parsons *et al.* (*18*).

to act as chelates; and 1,6-hexanediamine, which most often acts as a monodentate ligand. The possibility of one diamine molecule bridging between two sites must also be considered (*11*). Figure 1 illustrates these possible coordination modes for en bonding to the idealized (0001) Cd-rich face of CdS or CdSe, the surface used in our experiments (*12*). As a basis for comparison, we also examined several sterically and electronically related monoamines: *n*-propylamine, *n*-butylamine, *n*-heptylamine, aniline, and *o*-toluidine (*o*-methylaniline) (*13*).

In a typical experiment, the red band-edge PL of CdSe (720 nm; bandgap energy $E_g \sim 1.7$ eV) or green band-edge PL of CdS (510 nm; $E_g \sim 2.4$ eV) is excited with ultra-bandgap light while the sample is immersed in cyclohexane solvent (the reference state) or in cyclohexane amine solutions; the liquids are easily changed without altering the sample-detection optics geometry (*14*). The intensity of the PL is reversibly enhanced relative to its value in pure cyclohexane by exposure to amines; the enhancement increases with amine concentration and eventually saturates (*15*) (Fig. 2). The maximum enhancement can be used to estimate the maximum change in the semiconductor's depletion width resulting from adduct formation, by means of a dead-layer model. A key feature of the model is that electron-hole pairs formed within a distance from the surface on the order of the depletion width do not contribute to PL because they are swept apart by the electric field (*16, 17*).

The quantitative form of the dead-layer model is given by Eq. 3,

$$PL_1/PL_2 = \exp(-\alpha'\Delta D) \qquad (3)$$

where PL_1 is the PL intensity in cyclohexane solution; PL_2 is the PL intensity in amine solution; $\alpha' = (\alpha + \beta)$ is the sum of the semiconductor absorptivities for the exciting and emitted light (*18*); and ΔD is the contraction in the nonemissive dead layer, assumed to approximate the change in depletion width that occurs as the solution changes from pure cyclohexane to the amine solution. An operational test of the dead-layer model is to excite with several different interrogating wavelengths: α' and the corresponding PL ratios will vary, but ΔD, when calculated, should remain constant. Use of the dead-layer model assumes that the surface recombination velocity S is either insensitive to the ambient or very large in both ambients [$S >> L_p/\tau_p$ and $S >> \alpha L_p^2/\tau_p$, where τ_p and L_p are the minority carrier (hole) lifetime and diffusion length, respectively] (*19*).

Qualitatively, the direction of the amine-induced PL changes matches that found with gaseous amines (*2*) and defines a "luminescent litmus test." Because the depletion width was formed by the withdrawal of electron density from the solid's bulk, Lewis bases that can donate electron density to the semiconductor are expected to shrink the depletion width and thus to increase PL intensity; conversely, electron-withdrawing Lewis acids should increase the depletion width and reduce PL intensity (*20*).

The dead-layer model can be applied quantitatively to amine adsorption onto CdSe. Data obtained with a single CdSe sample reveals that for each of the amines the triad of laser lines used does give a roughly constant value of ΔD (*21*) (Fig. 3). The responses observed serve to separate potentially chelating from nonchelating amines. All of the aliphatic monoamines along with tn and 1,6-hexanediamine gave similar ΔD values of ~350 Å, but the potentially chelating en gave a much smaller value of ~150 Å. Similarly, the aromatic amines aniline and *o*-toluidine gave values for ΔD of ~450 Å, but opda, the potential chelator, gave a substantially reduced value for ΔD of ~250 Å. The amines also caused enhancements in the PL from CdS (450-nm excitation) with identical chelate versus nonchelate categorization. The greater depletion-width contractions for the aromatic monoamines parallel their lower ionization potentials relative to the aliphatic monoamines (*3, 22*).

It may be argued that, rather than being attributable to chelation, the reduced values of ΔD observed for en and opda could be due to exclusively monodentate coordination at lower surface coverages relative to the other amines. The steric pairings used suggest that this is an unlikely scenario. Each of the diamines has a monoamine counterpart of similar molecular size, yet only for en and opda do we see a reduction from the ΔD value of the monoamine partner. We eliminated opda from consideration as a bridging ligand, which could also lead to reduced coverage, on the basis of the calculated distances between two adjacent Cd^{2+} lattice sites of ~4.3 Å for CdSe and ~4.1 Å for CdS (*23*), which are too far for opda to span (*24*). The similarity in PL responses between en and opda, coupled with en's propensity for chelation, suggests that the bridging mode of coordination is unlikely for en as well.

If we take these data collectively, the anomalous en and opda ΔD values suggest that their binding is intrinsically different. Presuming that the difference reflects chelation, we can think of at least two reasons for the smaller perturbation of the semiconductor's depletion by a chelate. One possibility is that en and opda may be present at smaller absolute coverages, thereby attenuating the effect on the depletion width. There may be fewer of the doubly substitution-labile surface sites available for chelation, limiting the number of adsorbed en and opda molecules relative to the other amines; monodentate adsorption of en and opda at the remaining surface sites might be minimized by the engagement of en and opda in intramolecular hydrogen bonding in nonpolar solvents (*25*). Another possibility is that chelation may simply produce a smaller electronic perturbation. Absolute surface coverages, not obtainable from these PL data, are needed to evaluate these possibilities. The fact that the same trends are observed for both CdS and CdSe is consistent with the use of a similar binding site on each substrate, presumably surface-lattice Cd^{2+} sites.

The chelate effect should also be evidenced by comparisons of adduct equilibrium constants. Concentration-dependent PL changes can be fitted by means of the Langmuir adsorption isotherm model to obtain these constants (*2–5, 26, 27*). In this model, the fractional surface coverage θ [assumed to equal the fractional PL change (*28*)] depends on the amine concentration *C* and the equilibrium constant for adduct formation *K*:

$$\theta = KC/(1 + KC) \text{ or } 1/\theta = 1 + 1/(KC) \quad (4)$$

Thus a double reciprocal plot of 1/θ versus 1/*C* should be linear with an intercept of unity and a slope of 1/*K*.

We find that Eq. 4 gives excellent fits to our data (with all intercepts between 0.9 and 1.1). Plots for two of the compounds are displayed in Fig. 4. Calculated values of *K* for the CdS/amine and CdSe/amine adducts are given in Fig. 5. The equilibrium constants for the en and opda adducts are roughly two orders of magnitude larger than those of the other amines, providing compelling evidence for the chelation of these diamines to the surfaces of CdS and of CdS(e) (*29*). The trend in *K* parallels the enhancement in equilibrium constant seen in aqueous solution for Cd^{2+} in the presence of monoamines and en (*7*). Interestingly, tn, as it does in aqueous solution, exhibits a value of *K* intermediate between those of en and the monoamines, perhaps reflecting the reduced stability of six-membered chelate rings as compared to five-membered rings (*6*), or a mixture of binding modes, or both. Competition experiments affirm the ordering of the equilibrium constants and demonstrate that chelating diamines and monoamines compete for surface sites. For example, one observes an intermediate PL enhancement relative to those found separately with opda and aniline by adding to the cell, in either order, a dilute (2 m*M*) opda solution and a concentrated (200 m*M*) aniline solution. It is noteworthy, too, that the adduct equilibrium constants are relatively insensitive to the choice of CdS or CdSe substrate, consistent with the notion that Cd^{2+} surface ions serve as the monodentate and bidentate binding sites.

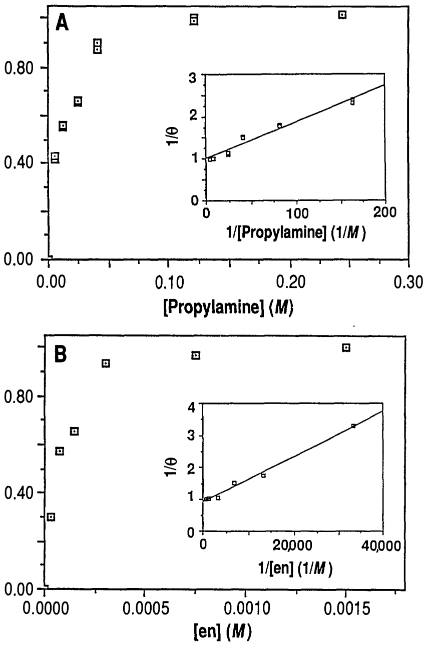

Fig. 4. Plots of θ (assumed to be equal to the fractional PL change resulting from 457.9-nm excitation) versus concentration for the adsorption of two of the amines studied, (**A**) *n*-propylamine and (**B**) en, onto CdSe; the double-reciprocal plots are shown as insets. From these experiments, log *K* for *n*-propylamine is ~2.1; log *K* for en is ~4.2.

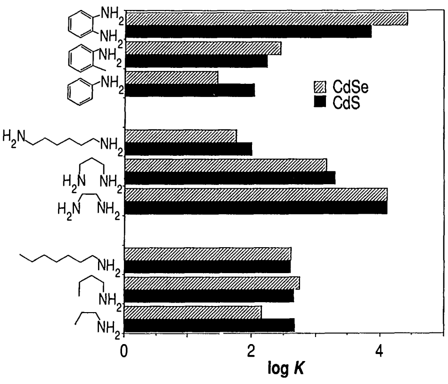

Fig. 5. Calculated values of log *K* for the interaction of the indicated amines with single samples of CdS and of CdSe. A pooled estimate of the standard deviation in log *K* is 0.1 (20 df). The CdSe data were determined for the same sample as in Fig. 3.

Note added in proof: Chelation at the surface of colloidal TiO_2 has also been reported recently (*30*).

REFERENCES AND NOTES

1. E. Yablonovitch, *Science* **246**, 347 (1989).
2. G. J. Meyer, G. C. Lisensky, A. B. Ellis, *J. Am. Chem. Soc.* **110**, 4914 (1988).
3. G. J. Meyer *et al.*, *ibid.* **111**, 5146 (1989).
4. C. J. Murphy and A. B. Ellis, *J. Phys. Chem.*, in press.
5. ———, *Polyhedron*, in press.
6. J. E. Huheey, *Inorganic Chemistry* (Harper & Row, New York, ed. 3, 1983), pp. 527–530.
7. D. D. Perrin, Ed., *Stability Constants of Metal-Ion Compounds*, Part B: *Organic Ligands* (Pergamon, Oxford, 1979).
8. A. Kozawa, *J. Electrochem. Soc.* **106**, 552 (1959).
9. J. W. Thackeray *et al.*, *J. Am. Chem. Soc.* **108**, 3570 (1986); T. Uchihara, M. Matsumura, J. Ono, H. Tsubomura, *J. Phys. Chem.* **94**, 415 (1990).
10. S. J. Fonash, *Solar Cell Device Physics* (Academic Press, New York, 1981), pp. 75–110.
11. W. P. Griffith, N. T. McManus, A. C. Skapski, *J. Chem. Soc. Chem. Commun.* (1984), p. 434.
12. Single-crystal, vapor-grown, samples of n-CdS (~10 ppm Te-doped) and n-CdSe, resistivity ~2 ohm-cm, were obtained from Cleveland Crystals. The crystals were etched in Br_2/methanol (1:30 by volume; 5 s) or concentrated HCl (5 s; methanol rinse), revealing the shiny 0001 face, which was excited in the PL experiments (see Fig. 1).
13. All of the amines are at least 98% pure as purchased from Aldrich and were distilled over KOH or recrystallized from ethanol before use. Cyclohexane (EM Science; <0.02% water) was purged with N_2. Solutions ranging from 1 μ*M* to 0.2*M* in amine were prepared and stored in a N_2 glove bag and used within 48 hours. Data for en were the most difficult to obtain, because of its sensitivity to water and the low concentrations used.
14. The sample cell consists of a glass tube 1 cm in diameter, with a Teflon stopcock at its bottom for liquid drainage; the semiconductor is glued with black epoxy to a glass rod and held in a Teflon adapter that serves as a stopper for the cell. A glass syringe, inserted through a side arm against positive N_2 pressure, was used to rinse the sample and fill the cell. Mounted samples were stored in cyclohexane in a N_2 glove bag when not in use. The CdSe samples were placed in a round sample cell and excited with a Coherent Innova 90-5 Ar^+ laser (457.9 and 514.5 nm) or a Melles-Griot model 80 helium-neon laser (632.8 nm), as described by Meyer *et al.* (*2*). The CdS samples were placed in a square sample cell in a Shimadzu RF-5000 fluorimeter and excited at 450 nm with the instrument's 150-W xenon arc lamp. With both setups, PL intensity was continuously monitored at the PL band maximum (a recorder was used in time-base mode) as the solution was varied. The cell was drained and the PL recorded in pure cyclohexane between each pair of measurements in amine solution. Measurements were made at ambient temperature; with the low incident powers used (<1 mW/cm^2), sample heating was negligible.
15. The magnitude of the PL responses depends on the surface condition. Sometimes the PL responses were sluggish after storage. The original response was then restored by re-etching, occasionally with the switching of etchants.
16. R. E. Hollingsworth and J. R. Sites, *J. Appl. Phys.* **53**, 5357 (1982) and references therein.
17. A. B. Ellis, in *Chemistry and Structure at Interfaces: New Laser and Optical Techniques*, R. B. Hall and A. B. Ellis, Eds. (VCH, Deerfield Beach, FL, 1986), chap. 6.
18. R. B. Parsons, W. Wardzynski, A. D. Yoffe, *Proc. R. Soc. London Ser. A* **262**, 120 (1961).
19. K. Mettler, *Appl. Phys.* **12**, 75 (1977); A. A. Burk, Jr. *et al.*, *J. Appl. Phys.* **59**, 1621 (1986).
20. P. C. Stair, *J. Am. Chem. Soc.* **104**, 4045 (1982).
21. The absorptivities for CdSe span a factor of 3 for the wavelengths in Fig. 3; the literature ultrabandgap absorptivity range is much smaller for CdS, providing a less critical test of the dead-layer model: D. Dutton, *Phys. Rev.* **112**, 785 (1958). The amines studied do not appreciably absorb at these laser wavelengths.
22. K. Watanabe and J. R. Mottl, *J. Chem. Phys.* **26**, 1773 (1957).
23. Calculated from data in W. R. Cook, Jr., *J. Am. Ceram. Soc.* **51**, 518 (1968).
24. R. C. Elder, D. Koran, H. B. Mark, Jr., *Inorg. Chem.* **13**, 1644 (1974).
25. P. J. Krueger, *Can. J. Chem.* **45**, 2135 (1967); *ibid.*, p. 2143.
26. T. Dannhauser *et al.*, *J. Phys. Chem.* **90**, 6074 (1986); T. Takeda and S. Okazaki, *Nippon Kagaku Kaishi* **5**, 608 (1983).
27. K. J. Laidler, *Chemical Kinetics* (Harper & Row, New York, ed. 3, 1987), pp. 230–232.
28. Good fits to the Langmuir model can also be obtained by relating θ to the fractional change in *D*: $\theta = [\ln (PL_x/PL_1)/\ln (PL_2/PL_1)]$, where PL_x is an intermediate PL intensity. Values of log *K* obtained in this manner are uniformly larger by ~0.2. This alternate definition of θ will be discussed elsewhere.
29. We were concerned that, rather than being attributable to chelation, the differences in *K* were due to the lower solubility of the diamines in cyclohexane and, consequently, a higher affinity for the surface:

E. Gileadi, in *Electrosorption*, E. Gileadi, Ed. (Plenum, New York, 1967), chap 1. However, each of the chelating diamines has a nonchelating diamine counterpart with similar or smaller solubility. Thus, 1,6-hexanediamine is similar in solubility to en, but en has a much larger *K* value; and use of *p*-phenylenediamine, a less soluble isomer of opda that cannot chelate, yields PL changes that have not saturated by the solubility limit, evidencing a much smaller value for *K* than was found for opda.

30. H. Frei, D. J. Fitzmaurice, M. Grätzel, *Langmuir* **6**, 198 (1990).

31. We are grateful to the Pew Mid-States Science and Mathematics Consortium for summer support of G.C.L. and R.L.P., and to W. R. Grace and Company for support of C.J.M. as a 1989–1990 fellow. This work was supported by the Office of Naval Research and the 3M Company. We thank L. F. Dahl, D. F. Gaines, C. P. Casey, S. H. Langer, and P. M. Treichel, Jr., for helpful comments.

12 December 1989; accepted 1 March 1990

Proximal Cretaceous-Tertiary Boundary Impact Deposits in the Caribbean

ALAN R. HILDEBRAND AND WILLIAM V. BOYNTON

Trace element, isotopic, and mineralogic studies indicate that the proposed impact at the Cretaceous-Tertiary (K-T) boundary occurred in an ocean basin, although a minor component of continental material is required. The size and abundance of shocked minerals and the restricted geographic occurrence of the ejecta layer and impact-wave deposits suggest an impact between the Americas. Coarse boundary sediments at sites 151 and 153 in the Colombian Basin and 5- to 450-meter-thick boundary sediments in Cuba may be deposits of a giant wave produced by a nearby oceanic impact. On the southern peninsula of Haiti, a ~50-centimeter-thick ejecta layer occurs at the K-T boundary. This ejecta layer is ~25 times as thick as that at any known K-T site and suggests an impact site within ~1000 kilometers. Seismic reflection profiles suggest that a buried ~300-km-diameter candidate structure occurs in the Colombian Basin.

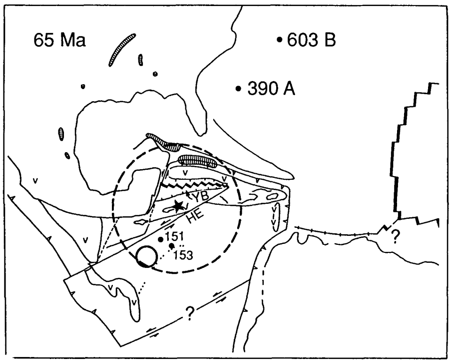

Fig. 1. A plate tectonic reconstruction of the Caribbean area at 65 million years ago [modified from (*43*)]; HE, Hess Escarpment; YB, Yucatan Basin. The lined areas show regions where impact-wave deposits occur. Impact-wave deposits also occur at DSDP sites 151, 153, and 603B. The star marks the position of the Beloc, Haiti localities. The dashed line is at a distance of 1000 km from those sites and corresponds to the inferred distance to the crater. The solid circle is a 300-km-diameter subcircular structure on the floor of the Colombian Basin. The positions of this structure and sites 151 and 153 and their distance to the Hess Escarpment and the Panama-Costa Rica arc have remained unchanged in this restoration. Oceanic crust south of the dotted line has since been subducted under South America.

ALTHOUGH AN ARRAY OF STRATIGRAPHIC, mineralogical, chemical, and isotopic evidence (*1*) has accumulated in support of the theory (*2*) that the Cretaceous Period was terminated by an impact of a large (~10 km) asteroid or comet, a suitable crater has not yet been found. Several craters with ages of ~65 million years are known (*3*), but they appear to be too small. The crater might have been destroyed, because half of the then existing ocean floor has been subsequently subducted (*4*). In this report, we (i) describe a thick ejecta unit and impact-wave deposits in the Caribbean that, in conjunction with stratigraphy at nearby sites, suggest that the impact occurred between North and South America, and (ii) identify a possible impact site in the Colombian Basin of the Caribbean Sea.

The clay layers at the K-T boundary compose a couplet. An upper layer ~3 mm thick occurs globally and contains anomalously large amounts of siderophile (*5*) and chalcophile (*6*) trace elements, shocked minerals (*7*), spherules with spinels (*8*), soot (*9*), isotopic anomalies (*10, 11*), and anomalously low amounts of incompatible lithophile elements like the rare-earth elements (REE) (*12, 13*). We call this the fireball layer, implying that it was dispersed by the impact fireball formed by vaporization of the projectile and target (*14*). On and near North America, a clay layer ~2 cm thick and containing similar evidence for an impact (*12, 15–18*) underlies the fireball layer. This layer (ejecta layer) may represent a geographically restricted facies of less energetic impact ejecta (*19*).

The Sm-Nd and Rb-Sr isotopic systematics and the incompatible trace element compositions of both layers (*11, 15, 20*) can be modeled as a mixture of ~20% oceanic crust, ~70% depleted mantle, and only ~10% continentally derived material (*12*). In addition, 10 to 15% of the fireball layer must be derived from an extraterrestrial object to account for its siderophile trace element abundances (*5*). The presence of pyroxene spherules and possibly shocked chromite grains in the fireball layer (*21*) is also suggestive of an oceanic impact site.

The occurrence of shocked and unshocked grains of quartz, alkali feldspar, and other felsic rock fragments in the fireball layer has often been cited as evidence of a continental impact (*7, 22*). However, the small amount [<1% globally averaged (*22*)] of such material is consistent with an impact into an ocean basin. The ejecta layer contains at least one order of magnitude fewer shocked felsic minerals than the fireball layer (*18*).

Three lines of evidence indicate that the K/T impact was located near, and probably between, North and South America:

1) The maximum concentration of shocked mineral grains and the largest grains occur in North America (*7, 22*).

2) Probable impact-wave deposits have been reported at the K-T boundary (*23, 24*) only from the Caribbean and southern North America. (Fig. 1). Coarse deposits occur from shallow water to outer shelf environments along the southern margin of North America. A coarse boundary deposit also occurs at a continental shelf boundary in New Jersey (*25*). Offshore, at DSDP site 603B on the continental rise, a turbidity current deposited or reworked the ejecta layer (*17, 26*). The thickest, impact-wave deposits may occur in western and central Cuba, where Pszczolkowski (*27*) described a single graded bed from 5 to 450 m in thickness, occurring across 500 km and containing 500 km^3 of sediment. The bed contains clasts up to 1.5 m in diameter at its base, many of which came from shallow water regimes, even though they were apparently deposited in a deep trough between the Bahamas platform and the Cuban island arc.

The only known abyssal K-T boundary sections showing coarse boundary deposits, which overlie stratigraphic gaps in the Upper Cretaceous, are DSDP sites 153 and 151 (Fig. 1) (*28*). At site 153, a ~15-cm-thick

---

Department of Planetary Sciences, University of Arizona, Tucson, AZ 85721.